8-6-2013

# Implementation and Application of the Response EAM for HCP Metals

Matthew J. Stagon
*University of Connecticut - Storrs*, matthew.stagon@gmail.com

# Implementation and Application of the Response EAM for HCP Metals

Matthew Joseph Stagon

B.S., University of Connecticut, 2011

A Thesis
Submitted in Partial Fulfillment of the
Requirements for the Degree of
Master of Science
at the
University of Connecticut
2013

# APPROVAL PAGE

Master of Science Thesis

# Implementation and Application of the Response EAM for HCP Metals

Presented by

Matthew Joseph Stagon, B.S. Civil Engineering

Major Advisor _____

Hanchen Huang

Associate Advisor _____

Jiong Tang

Associate Advisor _____

Eric Jordan

University of Connecticut

2013

# ACKNOWLEDGEMENTS

I would like to thank my advisor, Professor Hanchen Huang for his outstanding guidance and mentoring, my committee members, Jiong Tang and Eric Jordan, and my family for their continued support.

## TABLE OF CONTENTS

## TABLE OF FIGURES

# ABSTRACT

Atomistic simulations are a powerful tool for the study of materials, especially in the determination of underlying atomistic mechanisms. Molecular dynamics (MD) is an atomistic simulation method that is well suited for a large number of atoms in a system, up to one billion. MD holds sufficient physical rigor while keeping the number of calculations reasonable for modern computational power. In molecular dynamics, a mathematical potential is used to capture the physics of the interaction between two adjacent atoms or molecules. Existing potentials fail to adequately represent the interaction between some materials, such as Magnesium and Titanium, or are based off of non-physics based parameter fitting which suffers from a lack of rigor. For example, the potentials cannot accurately represent electron density distribution and therefore cannot properly replicate elastic constants and surface relaxation in Hexagonal close packed (HCP) materials and some Face centered Cubic Materials (FCC). In this work, we first review the past 30 years of progress in atomistic simulation, more specifically molecular dynamics, discuss the issues with the existing interatomic potentials, and then establish the need for a new response interatomic potential, or the R-EAM. The R-EAM is based on an approximate form of quantum mechanics theory and is an extension of the existing Embedded Atom Model (EAM) potential. Further, we go on to show simulations to confirm the R-EAM by examining dislocation motion in Magnesium nanorods under tension. The $(10\bar{1}2)\,[10\bar{1}1]$ dislocation is found in the HCP material, Magnesium, in accordance with experiments. Further implementation of R-EAM should allow for great expansion of molecular

dynamics because of its increased accuracy in reproducing surface relaxation and dislocation dynamics for HCP and FCC metals.

# 1. INTRODUCTION

## *A. Motivation*

This section presents why we want to study materials and how the understanding of materials and their properties is the key to technological innovation. Without the understanding of materials and science based engineering, technological innovation becomes a game of guess and check, and is time consuming.

The study of materials is at the center of modern engineering science and technology. Within the study of materials, there are three main factors that engineers must understand: process, structure and properties. Simply, the processing of a material is what the material undergoes to become the end product, from ore to ingot. The structure of the material is how the atoms and molecules are arranged to compose the bulk. The properties of the material are intrinsic reactions of the material to different external stimuli. Examples of this are the strain when a stress is applied or the temperature profile when heat is supplied. However, a clear connection exists between all three. The process dictates the microstructure, or the arrangements of atoms and molecules, and the microstructure dictates the properties. As engineers it is critical to understand the properties of the materials that we use to create devices and processes. The properties can be studied on two levels. First, the properties may be studied experimentally; for example, the strength and thermal expansion of a titanium alloy bar or a titanium nanowire may be measured. Going deeper, second, the microstructure may be studied to understand what mechanisms on the atomic scale give rise to the observed

properties. For example, we may first understand that the strength of a material is derived from its resistance to the glide of dislocations through the crystal lattice[1]. We may go even further to determine how the surfaces of solid effect the mechanical strength which changes as a function of the thickness or diameter of specimen[2]. Therefore, to truly understand engineering materials and make future advances, we must investigate the microstructure of materials.

There are two ways to study materials, experiments and modeling, and each has its own strengths and weaknesses. First, in experiments we directly observe the behavior of physical matter. This means that, although there may be some artifact or our interpretation may be incorrect, what we are observing is always physically true. For example, we may directly study the diffraction pattern of a material to see its crystal structure. Experiments cannot solve all problems because of two key limitations. First, we can only observe things down to a certain level of smallness, below which we can no longer see[3]. For example, it is very difficult to see single atoms and perhaps impossible to see individual electrons directly; the wave nature of electrons is also much more prominent than that of atoms. Second, experiments are very costly and time consuming. For example, if we want to study radiation damage we must have a dangerous radiation source that requires expensive shielding and if we want to study 500 different materials we must either have a person prepare each sample or create a sophisticated enough machine to take the place of the person. In this regard, experiments are limited in what can be directly studied, how much can be studied and in what time frame. On the other hand, computer simulations work well in the areas that experiments do not, and lack in the areas that experiments are strong in. Unlike experiments, using computational modeling, it is possible to replicate the dangerous environment for radiation damage with only the cost of a personal

computer (PC). Further, it is possible to model a large number of things in parallel, leading to time savings compared to experiments. Alternatively, it is possible to miss important physical parameters in the computational model and create something that is unphysical. Overall, the combination of computational modeling and experiments allows for the fastest progress in understanding materials on the atomic scale.

Depending on the involved physics, computational models of materials may be on several different scales. First, a continuum model, such as a finite element representation, may be used to model macroscopic behavior of materials. On this scale, the model is based on a mathematical discretization of material geometry and the reaction of the material to external load- mechanical, thermal or chemical- is based on a mathematical model of this property which may or may not contain rigorous physics. This scale of modeling is well suited for solving classical engineering problems. A level lower, there are atomistic simulations which look at atom dynamics in crystal structures. On the high level is lattice kinetic Monte Carlo (LKMC) simulations which model materials using the Monte Carlo prediction method and have a prescribed inter-atomic interaction which does not contain a large amount of physical rigor in exchange for time. In LKMC, the laboratory time scale may be simulated and processes like growth of thin films may be modeled. A level deeper and including more physics is molecular dynamics. Molecular dynamics relies on a detailed interatomic potential approximation between atoms. Due to the computational rigor involved, molecular dynamics is limited to only systems on the order of $10^9$ atoms on the time scale of nanoseconds. Going to the base level, first principles calculations take into effect the most rigor and rely on quantum mechanics. With these calculations, only 10s or 100s of atoms may be used at extreme computational cost.

Molecular dynamics is well suited for the study of materials on the atomistic scale as it has appropriate physical rigor and moderate computational cost. Unlike first principles calculations, molecular dynamics allows the study of systems that approach several nanometers.

### *B. What is Molecular Dynamics?*

Molecular Dynamics (MD) is a computationally efficient and fast approximation of the quantum mechanics description of atomic interactions[4]. It is based on the wave function solution to the Schrödinger partial differential equation[5]. Whereas the wave function must take into account spatial positions of electrons over time, molecular dynamics assumes the electrons move instantaneously relative to the core atomic nuclei; this is known as the Born–Oppenheimer approximation[6]. The atomic nuclei may then be assumed to be a point mass with velocity, acceleration and rotation of that of a standard particle in Newtonian mechanics.

In order to obtain a better understanding of the power of molecular dynamics, a comparison must be made between other computational methods for their overall efficiency and accuracy. Kinetic Monte Carlo simulations are a viable alternative to molecular dynamics in terms of computational speed[7]. Events are guided by random number generating algorithms. Atomic diffusion and interactions are based on probability distributions of certain events occurring at any time. This allows for simulations on the magnitude of $10^{23}$ particles and a timeframe of seconds, representing real world processes. Overall mechanisms for thin film growth, and equilibrium material properties are represented accurately on average over time with KMC. However in KMC, dislocation dynamics on the atomic scale and any discreet snapshot of atomic movement is ultimately meaningless.

Quantum mechanics seeks to mathematically to define the interactions of material on the atomic and subatomic, directly taking into account electron position and motion. The Schrödinger equation in quantum mechanics serves as an analog to the Newtonian equation of motion for three dimensional space. The Schrödinger equation is a partial differential equation which describes a spectrum of particles position over time. The solution to the Schrödinger equation can be used to define the probability distribution of a particle, and its likelihood to be in a location for a specified time. However, the solution to the Schrödinger equation does not have a finite domain and is computational expensive to obtain accurate results for large scale atomic simulations.

Molecular dynamics holds supremacy for simulating the underlying mechanisms for nano-scale physical phenomena in the world. MD enables direct observation of these events at an achievable speed with relatively resource sparing computational calculations.

### *C. Formulation*

Before presenting the new work in the implementation of the REAM, we must first describe the formulation of molecular dynamics, then move forward to the formulation of inter-atomic potentials to provide the reader with the necessary background. Molecular dynamics is derived from newton's laws of motion for a point mass. Newton's second law states that the acceleration of a body is proportional to the external force acting on the object and object's mass[8].

$$\boldsymbol{F = ma = m\frac{d^2x}{dt^2}} \tag{1}$$

Through the integration of the equation above with respect to time, one obtains equations for the velocity and position of a particle. An extension of newton's second law includes the torque experienced by the rigid body,

$$\boldsymbol{T = \vec{r}\, x\, \vec{F} = \vec{r}\, x\, m\vec{a} = \frac{dL}{dt} = I\alpha} \tag{2}$$

Integration of the equation of torque with respect to time results in relationships for angular velocity and rotation. Together these equations provide a complete description of a particle's translation and rotation over time.

Real solids however are not points but deformable volumes. Expanding on newton's laws, one arrives at the idea of a continuum solid[9]. A continuum solid can be seen as the division of a bulk material into sufficiently small neighboring elements. Each element in the continuum is capable of a relative displacement and hence the solid as a whole may experience a strain and stress. Continuum mechanics relies on the following basic principles: 1) properties are uniform within each element. 2) The element's material properties remain uniform as their size approaches infinitesimal proportions. 3) Such an element follows the equations of motion of a rigid body and newton's third law with nearby particles. 4) The solid follows the principles of conservation of mass and is continuous; hence no fractures may be present. Since each element in the continuum behaves according to Newtonian laws and element properties may be described using standard engineering descriptions for resistance to shear and normal stress. Continuum mechanics accurately reproduces bulk material characteristics; however it has difficulty in inaccurately predicting material properties as finite volume approaches zero. This is due to the fact that any material is composed of atoms, and hence a finite volume cannot be

smaller than atomic volume without knowing nuclear forces. Additionally, electrons in space are located in a non-uniform distribution and have no sharp ending point.

Molecular dynamics solves this problem by representing material on the individual atomic scale. Atoms in a molecular simulation take the place of point masses in the Newtonian equation. Initial positions are defined by the natural lattice arrangement in real materials. Forces experienced between atoms are obtained from the gradient of a “potential”, a function which approximates electron distribution and core nuclei repulsion.

# 2. ELEMENTS OF MOLECULAR DYNAMICS

## *D. Potentials*

Bonding in solids may take multiple forms ranging from covalent bonding to metallic bonding. In general bonding results from the sharing of electrons between atoms. So how does one go about accurately simulating bonding in solids? Electrons and atomic nuclei interact in an intricate fashion, forming a multi-body system. The Schrödinger equation is commonly used to describe atomic, molecular, subatomic, and various multi-body problems. The solution to the Schrödinger equation results in a wave function describing the quantum properties for a given element. However, the wave equation is difficult to solve for elements more complicated than a base Hydrogen atom from the resulting coupling between electrons and atomic nuclei. To decouple the wave function, one can assume that the lighter electrons move almost instantaneously to an equilibrium position relative to the speed of the much denser nuclei. This approximation reduces the wave function to the classical Newtonian equations of motion. Potentials fall into 2 general categories: simple pair interaction, and multi-body interaction. Pair interaction potentials take into account only the separation distance between single pairs of atoms. Multi-body potentials make use of higher orders terms which may depend on the total local electron density contribution, or angular dependence in relation to multiple atoms.

**Lennard-Jones (LJ)**

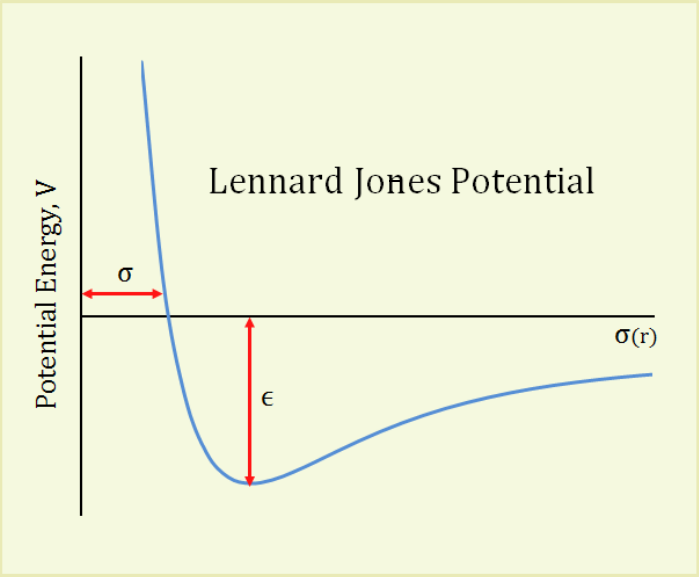


**Figure 1**

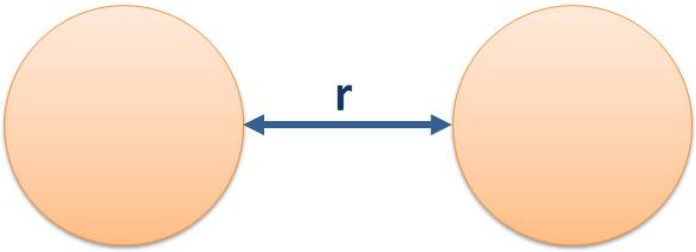


**Figure 2**

$$V_{LJ} = 4\varepsilon\left[\left(\frac{\sigma}{r}\right)^{12} - \left(\frac{\sigma}{r}\right)^{6}\right] \quad (3)$$

The Lennard-Jones potential is a classified as a simple pair potential. An initial form of the paper was drafted in the early 1920's by Jones[10]. Here r is the separation distance between atoms as seen in figure 2. σ is the separation distance at which the force between atomic pairs is zero, and $\varepsilon$ is the depth of the potential well seen in the figure 1. It found widespread use in

computational chemistry and physics in the early years of molecular dynamics because of its computational efficiency. It is a fairly accurate representation for noble gases and inert atoms or molecules; however it fails to represent more complicated systems with metallic or covalent bonding due to a lack of multi-body considerations.

**Embedded Atom Model (EAM)**

$$E_T = \sum_i E_i = \sum_i F(\bar{\rho}_i) + \frac{1}{2} \sum_{ij(i \neq j)} \varphi(r_{ij}) \tag{4}$$

$$\bar{\rho}_i = \sum_{j \neq i} \rho(r_{ij})$$

The embedded atom model is classified as a multi-body potential with local density dependence[11]. Here $E_T$ is the total energy of the system, which is the sum of energy contributions from each atom in the system. The total electron density, $\bar{\rho}_i$, is the sum of density contributions from nearby neighbors of atom i. Here $F(p)$ is the embedding energy, which can best be described as the energy required to place an impurity atom into an existing sea of electrons (figure 3). The function, F(p), generates a multi-body effect because of its dependence on the total local electron density of each atom.

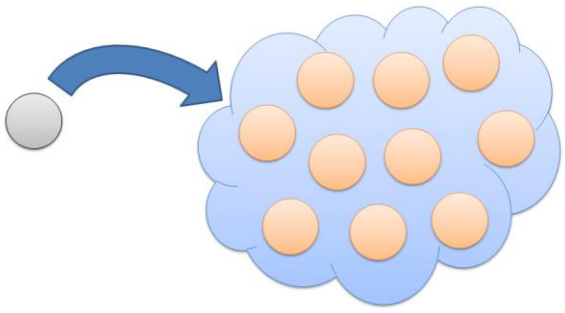

**Figure 3**

The function, $\varphi(r_{ij})$, is a pair interaction which represents the core repulsive forces experienced between atoms. The EAM is an improvement over existing atomic potentials such as the LJ potential, in that it considers multibody effects from atoms. Electron density is a summation over many neighboring atoms, and subsequently the total energy is dependent on this local density. This multi-body effect allows the embedded atom method to more accurately represent elastic constants. The previous limitations on basic pair interaction potentials such as $C_{12}$ equals $C_{44}$ no longer apply (reference). Additionally, surface relaxation and bonding is more accurately represented in terms of direction and magnitude (reference).

### *E. Time Integration*

Molecular dynamics programs make use of numerical time integrators in order to obtain future linear and angular position, velocity, and acceleration of particles. Some commonly used algorithms are the Verlet and gear approximation. To derive the Verlet method for time integration, we start with the basic Newtonian equations of motion.

$$F(t) = m\ddot{x}(t) \tag{5}$$

One can approximate the second derivative of position with respect to time by using a central difference approximation. Assuming a constant timestep and mass, the acceleration of a particle is written as the following

$$\ddot{x}(t) = \frac{\frac{x_{n+1} - x_n}{\Delta t} - \frac{x_n - x_{n-1}}{\Delta t}}{\Delta t} = \frac{x_{n+1} - 2x_n + x_{n-1}}{\Delta t^2} \tag{6}$$

From the above equation for acceleration one can determine the future position of the particle using only the current position, the previous position, and the force exerted on the particle.

$$x_{n+1} = \ddot{x}(t)\Delta t^2 + 2x_n - x_{n-1} = \frac{F(t)}{m}\Delta t^2 + 2x_n - x_{n-1} \quad (7)$$

A more commonly used offshoot of the Verlet algorithm is the Velocity Verlet. The Velocity Verlet computes both position and velocity in the same time step thereby saving computational resources[12].

However, all numerical time integration produces errors of varying magnitude. In order to minimize these errors, a sufficiently small time step may be chosen for a simulation run at the expense of computational time. The proper time step should be sufficiently small to observe the vibration and diffusion of the given material. Values for typical time steps can range of 5%-10% of the vibrational period, for example 1 femtosecond for metals[13]. Regardless of the time step chosen the magnitude of errors will become sufficiently large with time. Fortunately to make use of these simulations, one can assume that the error does not affect the base underlying mechanisms.

### *F. Neighbor lists, Domain lists, and cutoff*

In order to perform calculations in an efficient matter, force calculations between atoms beyond a chosen cutoff distance are assumed to be zero (figure 4). A list of neighbors with this cutoff distance is built for each atom within the system and these lists are then used to perform force calculations. This approximation ensures that computation power is only used on nearby neighbors, as the number of calculations that would be performed will become increasingly

large with system size on the order N^2. However, this introduces a new problem in that one would need to calculate the distance between atoms in order to be able to determine which atoms are nearby or local to any given atom. To solve this problem, atoms with cutoff plus an addition “skin” distance are used to create neighbor lists. This assumption holds for stable NVE systems since atomic diffusion and vibration is relatively small. Larger skin distances and a smaller time intervals for neighbor list updates may be needed for simulations on radiation damage or particle bombardment. This allows the neighbors lists to be updated less often, increasing computation speed.

Domain lists is an algorithm, similar to that of neighbor lists, used to find adjacent atomic neighbors but through the use of simulation cell division. The simulation as a whole is divided into distinct cell volumes in n dimensions. The length of an edge of a given cell volume is chosen to be greater than the cutoff. The atoms in the system are sorted into their correct cell and then only nearby cells must be check for pair interactions[14].

The combination of domain lists with neighbor list results in the most computational efficient algorithm. Domain lists are used to quickly sort atoms within their own cells, and then neighbor lists are used to check whether within range of cutoff.

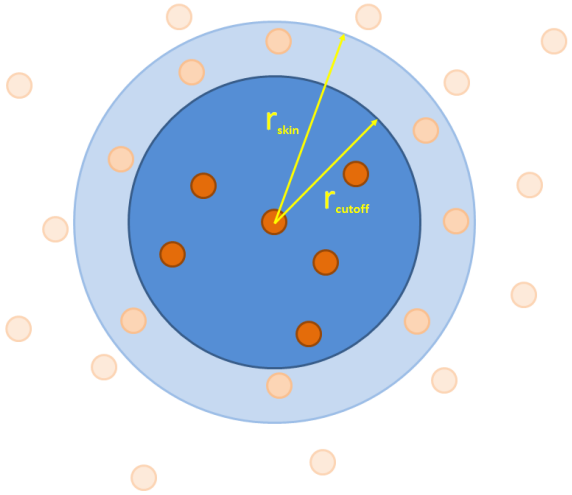


**Figure 4**

### *G. Conjugate Gradient Minimization*

Conjugate gradient method is an iterative algorithm used to obtain a solution to a complicated multiple degree freedom system. In the case of a molecular statics simulation, a large system of interconnected atomic positions must be solved for their optimum positions[15]. Conjugant gradient minimization may be used for simulating instantaneous quenching of system, and elastic constant and strength evaluation. The optimum configuration of the system may be found through energy minimization. The theory lies in the assumption that moving proportion to the steepest direction of descent will lead to the minimum energy state of the system. For a system of atoms the force or gradient of potential for each individual atom may be used. For an atom with position, r, its future position for time, t, is found by moving proportional to the direction of the deepest descent or gradient of the total energy of the system.

First the steepest descent direction is determined as gradient of the total energy of the system

$$\Delta \mathrm{r}^t = \nabla_{r_i^{t-1}} E_{Total} \tag{8}$$

Then a parameter $\beta$ for descent, known as the Fletcher-Reeves formula[16], is chosen as dot product of ration of the previous and current positions

$$\beta^t = \frac{\Delta \mathrm{r}^{t^T} * \Delta \mathrm{r}^t}{\Delta \mathrm{r}^{t-1^T} * \Delta \mathrm{r}^{t-1}} \tag{9}$$

The magnitude and direction of descent is then found to be

$$F^t = \Delta \mathrm{r}^t + \beta^t F^{t-1} \tag{10}$$

Next the line search parameter, $\propto$ is found through obtaining the minimum of the one dimensional function

$$\propto^t = min\ \mathrm{E}(r_i^t + \propto^{t-1} F^t) \tag{11}$$

Finally the position of the atom is updated as

$$r_i^t = r_i^{t-1} + \propto^{t-1} F^{t-1} \tag{12}$$

Initial values are set for the line search parameter and the descent path, as usually 0.1 and 0 respectively.

### *H. Boundary Conditions*

Fixed and free boundary conditions greatly affect the forces acting on a system, and the displacement experienced by the solid material, as in general solid mechanics problems for

continuous beams. A fixed end denotes a surface of an object which is immovable in terms of translation and rotation. A free end denotes a surface of an object which has the ability to move without resistance; it is traction free and has no stress component normal to the surface. To demonstrate the similarities and differences between continuous models and molecular dynamics, below is a cantilever beam (figure 5), point A designates the fixed end and point B the free end. The scale of a typical continuous model allows for approximations to be made for local stresses near applied loads. When a beam is under axial load the stress will be on average equal to P/A when far from the load site. However in molecular dynamics this assumption cannot be made due to surface effects. Additionally, representing axial tension is not as simple on the atomic level since it is unclear how to apply a load to individual atoms. A more accurate representation of axial tension would be based on uniform strain.

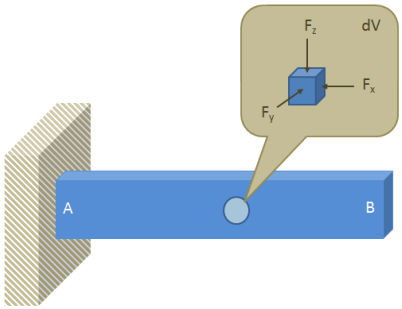


**Figure 5**

In molecular dynamics a fixed boundary condition can be represented by “freezing” groupings of atoms. These atoms are either not included in time integration or the forces experienced by these atoms are removed before subsequent calculations. The result is the same with atoms in a fixed group having neither translation nor rotation. A free surface is a group of atoms which

have no external load or modification of their movement. Free surface atoms are allowed to evolve naturally. This is analogous with fixed and free conditions in a continuous beam.

Molecular dynamics introduces a third boundary condition, a periodic boundary. A periodic boundary links opposite sides of simulation cell, so that they represent the same location. One can visualize periodic boundary conditions as picking a small ideal segment from a larger bulk, as seen in figure 5. Figure 6 depicts how an atom leaving the right border of the simulation cell reenters on the left border.

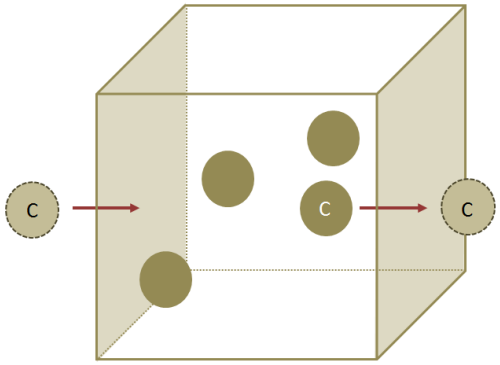


**Figure 6**

The proper boundary conditions in a molecular dynamics simulation must be carefully chosen to ensure realistic conditions and adequate computation speed. Current computational speed allows for simulations of 10^9 atoms, where as a real material has atoms on the order of 10^23 in number. To compensate for the unrealistic size of molecular dynamics simulations, one can use periodic boundary conditions. Periodic boundary conditions replicate the real simulation cell in all surrounding directions and these replicas act as the external environment for the true simulation cell. The simulation cell therefore interacts with itself, and in a sense is

comparable on average to a much larger cell of the same structure. It is important to note that periodic boundaries inherently enforce that the dimensions of the simulation cell must be greater than the cutoff distance of the potential in order to prevent atoms from interacting with their own "ghosts".

### *I. Thermostats:*

A thermostat is a form of self-governing control system which serves to maintain the temperature of a system at a desired level. It relates to the physical world, in that it seeks to replicate heat transfer in solids. For example one may wish to study a material's thermal conductivity on the atomic level, this can be achieved by holding the relative temperature of opposing ends of a long rod constant using a thermostat. The rod can then be modeled according to Fourier's law for heat flux.

$$\boldsymbol{q_x = -k\nabla T} \tag{13}$$

Temperature within a molecular dynamics abides by the ideal gas law

$$\boldsymbol{pV = nRT} \tag{14}$$

The ideal gas law can be reformulated in terms of the root mean square particle speed of the system.

$$\boldsymbol{\frac{1}{2}mv^2 = \frac{n}{2}k_bT} \tag{15}$$

Where m is the average mass of the particle, v is the root mean square speed of the system, $k_b$ is the Boltzmann constant, n is the degrees freedom of the system, and T is the temperature of the system

Temperature in a MD simulation may be maintained by multiple styles of thermostats, such as velocity rescaling, Berendsen ode (reference), or virtual particle interaction. In a system with a thermostat regulated with velocity scaling, particle velocities magnitudes are scaled but their relative velocities are conserved. The Berendsen thermostat results in a somewhat less severe approach to regulating temperature by using the ordinary differential equation[17]:

$$\frac{dT}{dt} = \left(\frac{T_0 - T}{w}\right) \tag{16}$$

The parameter w effects the rate of heat transfer occurring in the system.

However, both methods enforce an unrealistic distribution of particle velocities. Real systems display a Boltzmann distribution of particle speed proportional to $e^{-E/k_BT}$. The solution lies in a method proposed by Nose and Hoover, which is founded on the idea of a virtual particle exchanging energy with the system[18]. A Lagrangian for the virtual particle and each real atom is written for the entire system. The potential energy of the virtual particle is carefully chosen to form a canonical ensemble and is dependent on the number of degrees of freedom of the system. The end result is the following equation for atomic motion:

$$\ddot{x} = -\frac{k}{m}x - Q\dot{x} \tag{17}$$

$$\dot{Q} = \frac{1}{M}(m\dot{x}^2 - k_B T_0) \tag{18}$$

Here the mass of the virtual particle, M, dictates the rate of temperature change. Referring backing to the equation above relating particle velocity to temperature, one can see that when

the average kinetic energy of the system reaches that for the desired temperature, the friction coefficient Q becomes zero and the system is in stable equilibrium.

### *J. Barostats*

A barostat is a form of autonomous control system which serves to maintain the pressure of a system at a desired level. Before discussing the means for regulating pressure in a molecular dynamics simulation, one must have a way for defining stress on the atomic level. The atomic level stress of a system is founded on the virial theorem[19] and can be defined as

$$\boldsymbol{\sigma_{\alpha\beta}} = \frac{\mathbf{1}}{\boldsymbol{\Omega}}\left(\frac{\mathbf{1}}{\mathbf{2}}\sum_{\boldsymbol{i\neq j}}\left(\boldsymbol{r_j^{\propto}} - \boldsymbol{r_i^{\propto}}\right)\boldsymbol{f_{ij}^{\beta}} + \sum_{\boldsymbol{i}}\boldsymbol{m_i\dot{r}_i^{\alpha}\dot{r}_i^{\beta}}\right) \tag{19}$$

Where $\sigma_{\alpha\beta}$ is the component of the stress tensor in the basis direction $\alpha$ and $\beta$, $\Omega$ is the total system volume, $f_{ij}^{\alpha/\beta}$ is the projection of the interatomic force between atoms in the direction of one of the basis directions, $\dot{r}_i^{\alpha/\beta}$ is the projection of the current atom's velocity in one of the basis directions, and *m* is the mass of current atom. Here $f_{ij}^{\alpha/\beta}$ is obtained by taking the gradient of total potential energy of the system with respect to the basis vectors. The first term is essentially energy per projected area between atoms, analogous to the standard engineering definition of pressure. However the second term is a kinetic energy contribution imparted from atoms colliding with a virtual interface. Much controversy existed over whether the kinetic energy term is valid when compared to physical stresses experienced in a solid. Current

numerical simulations agree that the kinetic term is necessary for correctly reproducing the continuum mechanics concept of the Cauchy Stress tensor[20].

Given the idea of atomic Virial stress, one can now develop a means for controlling pressure in an MD simulation. This may be accomplished by artificial scaling the dimensions of the box with to obtain the desired external pressure using the Berendsen method previously noted for thermostats[17]:

$$\frac{d\sigma}{dt} = \left(\frac{\sigma_{external} - \sigma(t)}{w}\right) \tag{20}$$

Here once again w is the rate of pressure change, and convergence to the external stress. Without going into the details of derivation, the virtual particle method applied for thermostats can be applied in a similar format to barostats to obtain a lagrangian which allows for a natural particle velocity distribution and preservation of the canonical ensemble[18].

### *K. Thermodynamic Ensembles*

#### 1. Micro canonical (NVE)

In a micro canonical system, the number of atoms the volume of the system and the total energy remains constant. This represents a simulation say with periodic boundaries in all dimensions, with no thermostat present, and no incoming flux of atoms into the system. It is analogous to an isolated system with no heat transfer.

#### 2. Canonical (NVT, NPT)

In a canonical system, the number of atoms the volume of the system and the temperature remains constant. The total energy of the system is no longer required to be

conserved. A canonical system is analogous to a system with an efficient thermostat or barostat. For example under isobaric conditions the number of atoms, pressure and temperature remain constant for a solid. It is analogous to a situation in a pressure vessel is exposed to the atmosphere and ambient temperature.

3. **Grand Canonical (μVT)**

In a Grand Canonical system even the number of atoms is not conserved. It can be seen as a process in which a constant chemical potential, μ, is present. This process is represented physically as thermal evaporation or chemical reactions. Molecular dynamics is limited in its ability to simulate Grand Canonical ensembles.

## L. *Molecular Dynamics Program Outline*

A molecular dynamics simulation begins with the importation of initial condition data. The following information is imported at initial runtime: specification of the units of measurement of energy and distance, the size, degrees of freedom, and overall configuration of the simulation, the atomic postions, velocities and external forces of atoms, the potential used to define the attraction experience between atoms, and the intial kinetic energy of the system. A detailed schematic can be seen in Appendix A.

Then forces are calculated for each individial atom, obtained through the gradient from the given potential experienced by the atoms. Then boundary conditions are imposed through artificial conditions. Thermostats and barostats may be applied thereby scaling atomic velocities or box dimensions. Atomic positions may be fixed to simulate a rigid object. After all

artifical and internal conditions have been applied to the atom and forces have been calculated, a numerical time integration will be performed to obtain the future positions, velocities and accelerations of atoms within the system for a given timestep. Data is then exported to saved storage for later analysis. Analysis may include, elastic constant determination, dislocation studies, and various other phenomenon. If the simulation has reached the designated number of timesteps then the program ends, otherwise the loop continues.

### *M. Convergence*

For any simulation run using molecular dynamics one must make sure that the system is at equilibrium and not in a constant state a flux. A system in flux will be inherently unstable, proving in some cases impossible to reproduce by outside parties. Therefore all simulations performed were analyzed to ensure that they converged within a standard deviation over a given timeframe. Examples of convergence can be seen in Appendix A.

# 3. CRYSTALLOGRAPHY

### *N. Lattice*

A lattice is a repeating, usually symmetrical pattern of points. A lattice is synonymous to a vector space. Basis vectors for a vector space may be linearly combined to generate an endless number of points. These points make up the entirety of the lattice structure.

### *O. Unit cells*

Unit cells are the smallest possible volume which when replicated reproduces a given lattice for a material structure. Unit cells are composed of basis vectors and basis atoms. Basis vectors are a linearly independent set of vectors that when combined can be used to define any point in space. Any point or vector can be described as a combination of the unique basis vectors, allowing for efficient calculation and computations. For lattice space, one may define basis vectors: $\vec{a}$,$\vec{b}$, and $\vec{c}$. These vectors are not required to be orthogonal, nor are their lengths necessary equivalent; this will be seen later with the hexagonal close packed structure. So in general one may define α as the angle between $\vec{b}$ and $\vec{c}$, β as the angle between $\vec{a}$ and $\vec{c}$, and γ as the angle between $\vec{b}$, and $\vec{a}$. Basis atoms represent the points that will be replicated to form the lattice structure. They are described in terms of the chosen basis vectors and range from values between 0 and 1.

Many lattice structures exist for various materials, such as simple cubic, body centered cubic, face centered cubic, and hexagonal close packed.

The simple cubic crystal structure has equal basis lengths of a=b=c, and angles of α=β=γ=90°. The basis vectors are usually chosen to be parallel to the standard x, y, and z axis,

and therefore only one basis atom is needed to fully replicate the lattice. The basis atom may be chosen to be located at any corner point, due to symmetry. Very few applicable materials have simple cubic crystal structure.

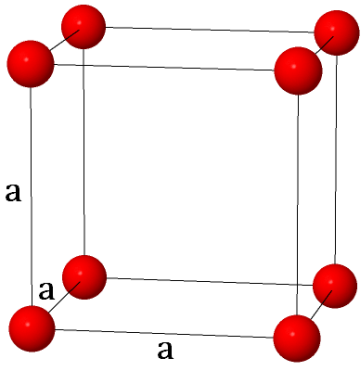


**Figure 7**

The body centered cubic crystal structure, like simple cubic, has equal basis lengths of a=b=c, and angles of α=β=γ=90°. The basis vectors are chosen to be identical to that of simple cubic as well. However two atoms are required to completely replicate the lattice structure. The basis atoms are located at a corner point, and the center of the unit cell. Common materials with BCC crystal structure are iron and Chromium.

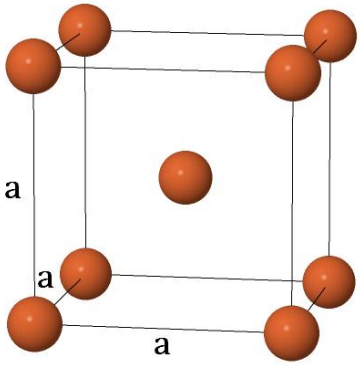


**Figure 8**

The face centered cubic crystal structure, has identical basis vectors and angles to that of simple cubic and body centered cubic. However, FCC has 3 basis atoms. The basis atoms are located at a corner point, and two faces of unit cell. Common materials with FCC crystal structure are gold and copper.

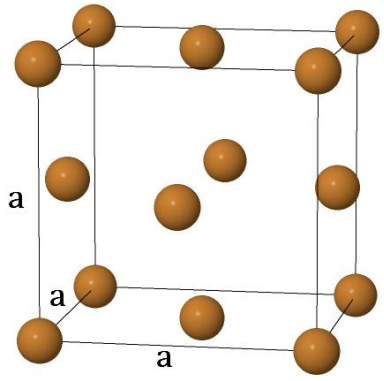


**Figure 9**

The hexagonal closed packed crystal structure is unlike any of the previous cubic lattices. HCP has equal basis lengths of a=b, with an independent length of c. The c direction is orthogonal to the vectors a and b with $\alpha=\beta=90°$, however the vectors a and b are separated by an angle $\gamma=120°$. The basis vectors are chosen to be points located at opposite corners of the hexagon structure as seen in the figure below. 4 atoms are required to completely replicate the lattice structure with this basis; 2 in plane and 2 out of plane. Common materials with HCP crystal structure are Magnesium, Titanium, Zinc.

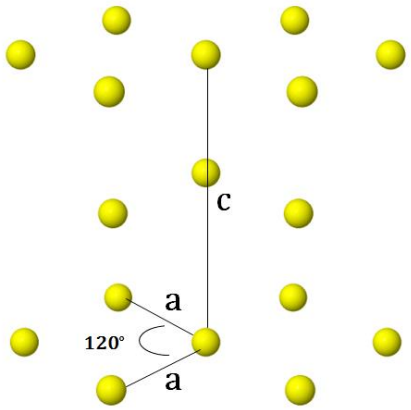


**Figure 10**

### *P. Miller Indices*

The Miller Index notation provides an easy method for defining crystallographic planes for any crystal structure, even one with non-orthogonal basis vectors. The general procedure for determining the miller indices is to find the points of intersection between the plane and the 3 basis vectors. Planes parallel to a basis vectors are taken as equivalent to infinity. Next one may take the inverse of the 3 intercepts previously found, and simplify the intercepts so as to have the smallest possible whole integer. These indices are displayed as (hkl) for 3 basis vectors respectively. Some common planes in cubic crystal systems are seen below

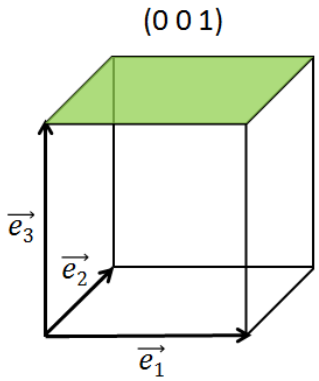


**Figure 11**

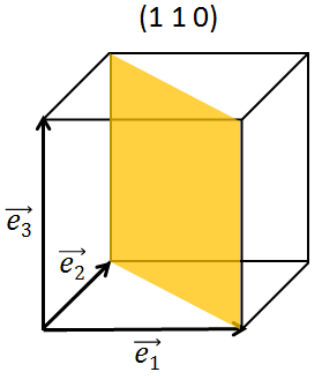


**Figure 12**

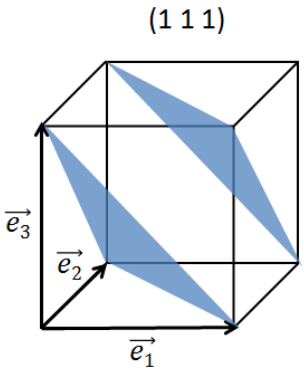


**Figure 13**

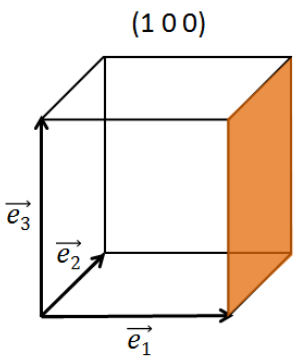


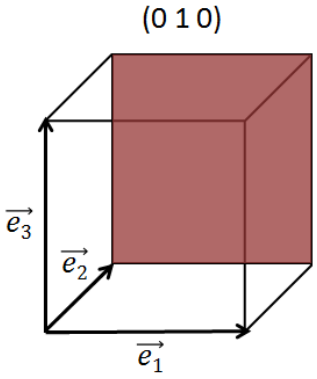


**Figure 14** **Figure 15**

For HCP there is an exception to the normal 3 miller index notation, with the addition of a 4th index. The 4 miller index notation references vectors $\vec{a}_1, \vec{a}_2, \vec{a}_3$and $\vec{c}$ which are represented by the notation (hkil). The vectors $\vec{a}_1$ and $\vec{a}_2$are equivalent to $\vec{a}$ and $\vec{b}$ as previous noted for HCP. A new vector $\vec{a}_3$, is generated which is equal to the combination, $\vec{a}_3$= -($\vec{a}_1$+$\vec{a}_2$). This new vector is given the miller index notation, $i = -(h + k)$. The overall miller index notation is denoted (hkil). Some common planes for the HCP structure are displayed below:

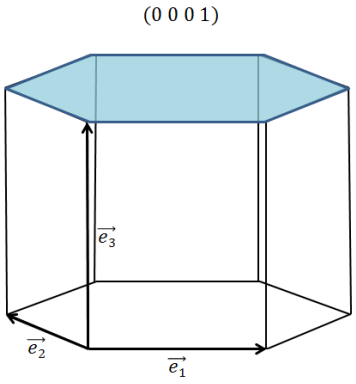


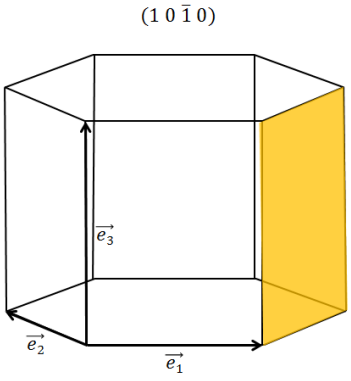


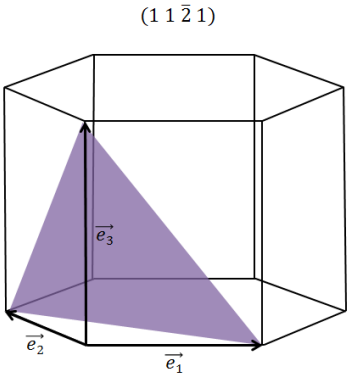


**Figure 16** **Figure 17** **Figure 18**

### *Q. Dislocations*

Dislocations are crystal defects, or irregular structures present in typical crystal lattices. Dislocations are generated when a solid is subjected to high levels of strain, resulting in plastic deformation. There are two types of dislocations, namely edge and screw. Real materials will contain a combination of both edge and screw dislocations (reference). An Edge dislocation occurs when a lattice structure is altered by the inclusion of an additional half plane of atoms between ideal planes. Screw dislocations can be seen as the result of the shearing of two partial cut segments of a lattice structure.

Slip planes are planes on which dislocations tend to move or grow in a given material, usually of the highest atomic packing density. Dislocations will move in preferred directions within the plane as well. The primary slip plane for HCP is (0001), (111) for FCC, (110) for BCC (reference). There are a limited number of slip systems in HCP with only one slip plane and three slip directions. Comparably, FCC has up to four slip planes and BCC has six slip planes. Slip of atomic planes and plastic deformation occurs when the system reaches the critical shear stress along the direction of the slip plane. For a solid under axial tension, the projected shear stress is

$$\boldsymbol{\tau = \sigma \cos(\varphi) \cos(\lambda)} \tag{21}$$

Here $\boldsymbol{\varphi}$ is the angle between the slip plane in question and the direction of applied load, and $\boldsymbol{\lambda}$ is the angle between slip direction and the applied load . The maximum shear stress will occur for the highest Schmid factor, dictated by $\boldsymbol{[\cos(\varphi)\cos(\lambda)]_{max}}$ (reference). The Slip system

with the highest Schmid factor will slip first. The Schmid factor is determined from the direct evaluation of the vector dot product for any slip system, or the combination of slip plane, $(h_1k_1l_1)$, and direction, $[h_2k_2l_2]$, and the applied load direction, $[a_1, a_2, a_3]$.

$$\boldsymbol{\cos(\varphi)\cos(\lambda) = \frac{(h_1k_1l_1) * [a_1, a_2, a_3]}{|(h_1k_1l_1)||[a_1, a_2, a_3]|} * \frac{[h_2k_2l_2] * [a_1, a_2, a_3]}{|[h_2k_2l_2]||[a_1, a_2, a_3]|}} \quad (22)$$

For example for the (111)/[1-10] slip system in FCC metals under an applied load in the [100] direction, the Schmid Factor is

$$\mathbf{M = \frac{(111) * [100]}{|(111)||[100]|} * \frac{[1\bar{1}0] * [100]}{|1\bar{1}0||[100]|} = \frac{1}{\sqrt{3}} * \frac{1}{\sqrt{2}} = \frac{1}{\sqrt{6}} = 0.408}$$

### *R. Strain hardening*

Plastic deformation of a solid leads to dislocations along slip planes. High levels of strain generate a very dense network of dislocations and grain mismatch creating a strengthening effect. Or in other words the creation of dislocations leads to a natural resistance to further deformation, known as strain hardening. Strain hardening can be used to increase the strength of many relatively ductile materials used for commercial applications such as carbon steel, copper and aluminum(reference). Therefore logically one can conclude that preventing dislocation mechanisms can create more ductile materials. The opposite could also be said for creating a more brittle material. However strain hardening can only be effective when obtained by plastically deforming a solid well below its melting point. If the stain hardening was attempted at high temperatures the high diffusion and local ordering would eliminate most dislocations and the beneficial strengthening effects.

Along the lines of preventing dislocation motion in order to strengthen materials one can add impurity atoms to a base solid generating an alloy. The impurity atoms create a local stress concentration as well as a lattice mismatch resulting in the cancellation of dislocation motion.

### *S. Twin Boundaries*

Twin boundaries grain boundaries along which lattice orientation and structures are mirrored on opposite sides. Two mirrored lattices share the same plane of points. Twin boundaries are most common in hexagonal close packed materials, and least common in face centered cubic and body centered cubic because of the number of slip systems present. HCP has very few slip systems whereas FCC and BCC have up to four or more (reference). Twin boundaries have a natural strengthening effect, which is why they are generated in HCP metals with few slip systems to increase strength.

# 4. CRYSTAL ANALYSIS TECHNIQUES

### *T. Burgers Vector*

The Burgers vector is a means a defining the magnitude of a dislocation occurring in a perfect crystal[21]. The burgers vector can be defined by visualizing a perfect rectangular loop dictated by the ideal atomic positions in lattice relative. When the ideal crystal is deformed so too is the rectangular loop. The resulting direction and length of deformation present in the rectangular loop is defined as the burgers vector, $\vec{b}$.

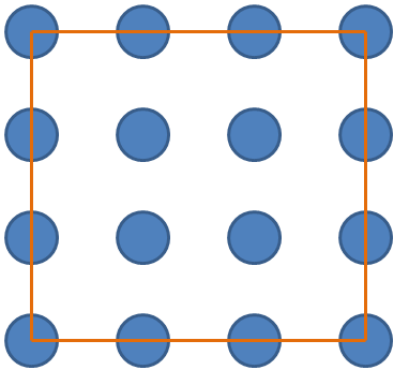

**Figure 19**

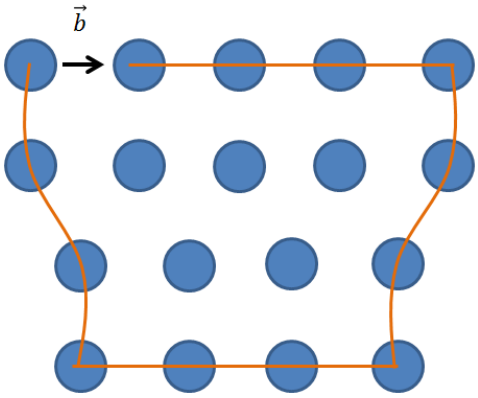


**Figure 20**

### *U. Radial Distribution Function*

The radial distribution function is a means for describing the local density a given distance r away from an average particle in the system[22]. It can be seen as the probability of finding a given density of atoms a distance relative from any atom, normalized by that typically found in an ideal gas.

### *V. Common Neighbor Analysis*

Common Neighbor Analysis (CNA) is a method used to characterize crystal structures and crystal defects. CNA is commonly used to distinguish between different crystal structures, and dislocation cores, surface adatoms, and atom clusters[23]. One begins by determining which surrounding atoms to classify as neighbors. The first local minimum of the radial distribution function for a given crystal structure is generally considered the neighbor cutoff. If two atoms are within this cutoff distance they are labeled as having formed a bond. Choosing a bond pair of atoms, one begins by finding neighbors which are common to the pair. The number of common pairs designates the first number in the common neighbor analysis notation. Next one determines the number of bonds formed between the common pairs, defining the second number in the common neighbor analysis notation. The final number in CNA notation is defined by the longest chain length created by the shared bonds.

# 5. R-EAM IMPLEMENTATION

### *W. Current Simulation Limitations*

Although the EAM reproduces experimentally determined properties for most metals fairly accurately, it fails to produce reliable results for some systems. Specifically the EAM imposes the following conditions: $C_{12}>C_{44}$ for cubic crystals[24], $C_{13}>C_{44}$ and (c) approximately $3C_{12}-C_{11}>2(C_{13}-C_{44})$ for hexagonal close packed (HCP) crystals[25]. It can be shown analytically that the R-EAM removes all of these constraints. The limitations on EAM potentials arise from the way that electron density contributions are distributed between atoms. In the EAM regardless of the local environment, as in the nearby atomic density, does not affect the relative distribution of electron density; each electron contribution from individual atoms is not affected by its neighbors. The R-EAM takes into account the local environment and allows for relative distribution of electron density. Historically, it has been shown that EAM fails to properly capture outward relaxtion in fcc metals[26]. Naturally, the response portion of the REAM and its relative electron distribution leads to a more accurate reproduction of surface relaxation. Interatomic spacing after relaxation, for the $(0001), (10\bar{1}0), (11\bar{2}0), (10\bar{1}1), \text{and } (10\bar{1}2)$ planes were compared between the Magnesium REAM, respected EAM potentials by Mishin and Liu, and quantum mechanics results. It was shown that the REAM has comparable direction and magnitude to that of quantum mechanics but the EAM has neither[27].

To present the REAM, we start with the framework of EAM.

$$\bar{\rho}_i = \sum_{j \neq i} \rho(r_{ij})$$

$$E = \sum_i E_i = \sum_i F(\bar{\rho}_i) + \frac{1}{2} \sum_{ij(i \neq j)} \varphi(r_{ij})$$

Here $E_T$ is the total energy of the system, which is the sum of energy contributions from each atom in the system. The total electron density, $\overline{\rho_i}$, is the sum of density contributions from nearby neighbors of atom i. $F(p)$ is the embedding energy, which can best be described as the energy required to place an impurity atom into an existing sea of electrons. Physically speaking, the electron density surrounding an atom will be distributed differently when nearby stronger bonding atoms or when situated within a larger number of neighbors. To account for this the total electron density may be written as the following:

$$\boldsymbol{\rho_R = \rho(r_{ij})[1 + R_j(\overline{\rho}_{ji})]} \tag{23}$$

The previous description of electron density would be extremely costly in terms of computational speed. Given that the subdivision of both embedding energy and pair interaction energy has multiple solutions, one may write the equation for electron density and atomic energy as the following:

$$\boldsymbol{E = \sum_i E_i = \sum_i F(\overline{\rho}_i) + \frac{1}{2}\sum_{ij(i\neq j)} \varphi(r_{ij})\,[1 + R(\overline{\rho}_{ji}, \overline{\rho}_{ij})]} \tag{24}$$

$$\boldsymbol{\overline{\rho}_{ji} = \overline{\rho}_j - \rho(r_{ij})} \tag{25}$$

Taking into account the symmetry of bonding for atoms i and j one may write the response function as a geometric mean of the coupled electron densities.

$$\boldsymbol{R(\overline{\rho}_{ji}, \overline{\rho}_{ij}) = R(\sqrt{\overline{\rho}_{ji}\overline{\rho}_{ij}})} \tag{26}$$

## X. *Implementation*

The molecular dynamics program LAMMPS[28], originally developed by the two national labs Sandia and LLNL, was extended with a R-EAM subroutine. The subroutine was inserted into the existing EAM multi-body potential present in LAMMPS architecture. The inner workings of LAMMPS and the placement of the R-EAM subroutine is visualized below, along with an outline of the coding methodology.

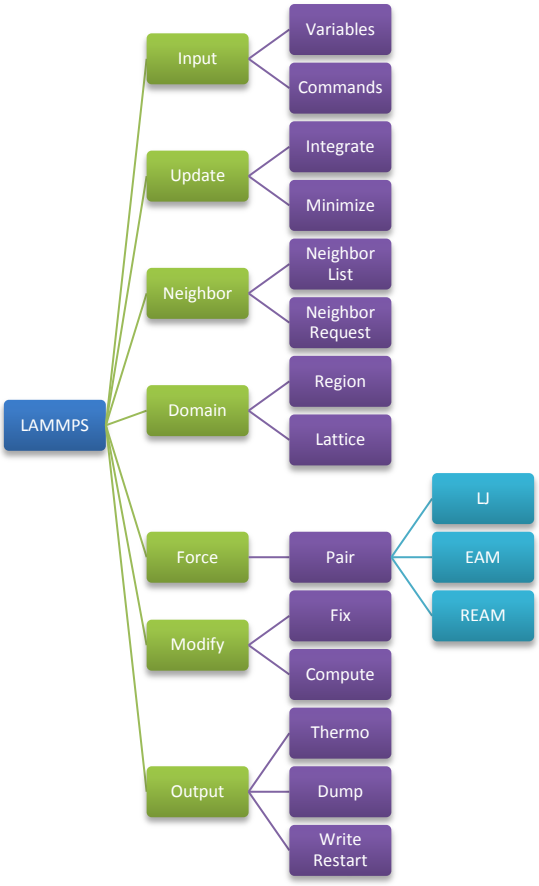


**Figure 21**

**Pair_REAM: compute() – PseudoCode**

---

1. Create arrays to store individual atom properties, and splined function values
2. Divide atoms and simulation cell between processors

3. Loops over neighbors j>i (in order to save computation time, since calculations are duplicate due to symmetry)
4. Communicate total electron density, electron density derivative, and embedding energy derivative
5. Compute energy contribution and net force per atom located on each processor
    a. Calculate embedding energy using total electron density
    b. Calculate the geometric mean of electron density between atomic pair
        i. Determine value for Response function using mean
    c. Calculate phi based upon separation distance
6. Sum forces and energy between processors

## *Y. Efficiency*

Before affirming the validity of the R-EAM, one must check the efficiency of the REAM relative to the existing EAM. If the REAM proves to be too computational expensive to be useful in common applications then it will fail to be more valuable than the existing EAM method. Simple simulations of bulk magnesium were carried out in LAMMPS, using the same Nose-Hoover temperature and pressure control, varying the number of processors used and the total number of atoms present in the system.

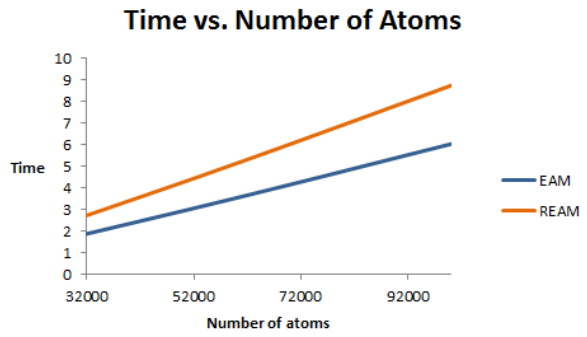


**Figure 22**

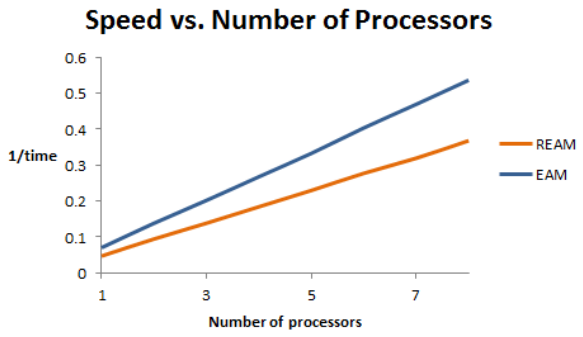


**Figure 23**

The results of these simulations show that on average the REAM is around 1.5 times slower than the EAM when it comes to computational speed for various system sizes; this holds true

regardless of the number of processors used. Important to note, the number of atoms used must never be smaller than 1000 atoms per processor to ensure efficient distribution amongst all nodes.

### *Z. Dislocation Motion*

**Figure 24**

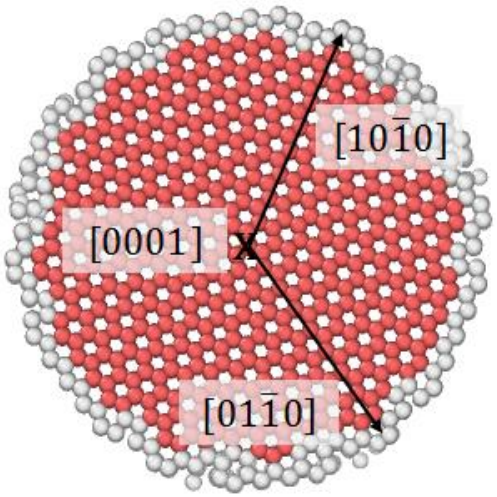


**Figure 25**

A simulation of a Magnesium nanorod under tension was run to test the strength, mechanisms for plastic deformation and the overall validity of the potential fitting. A 5 nanometer diameter and 30 nanometer long nanorod was generated in a 150 by 150 by 300 angstrom simulation cell with basis vectors $a_1 = a[1,0,0]$, $a_2 = a[0,\sqrt{3},0]$, $a_3 = c[0,0,1]$. Since the simulation was run at a nonzero temperature of 300 K, a finite temperature lattice value was used for quicker computation and more accurate atomic relaxation. Using an NPT barostat and thermostat a

bulk simulation cell was relaxed under isobaric conditions of 0 bars and 300 K, resulting in a finite temperature lattice value. The nanorod was also held at isobaric conditions for 100 picoseconds to allow for surface relaxation. The simulation cell was then deformed at a rate of $10^9\ s^{-1}$ and the atomic positions scaled relative to the deformation. The stress and strain values at .1 picoseconds increments were exported and graphed for data analysis.

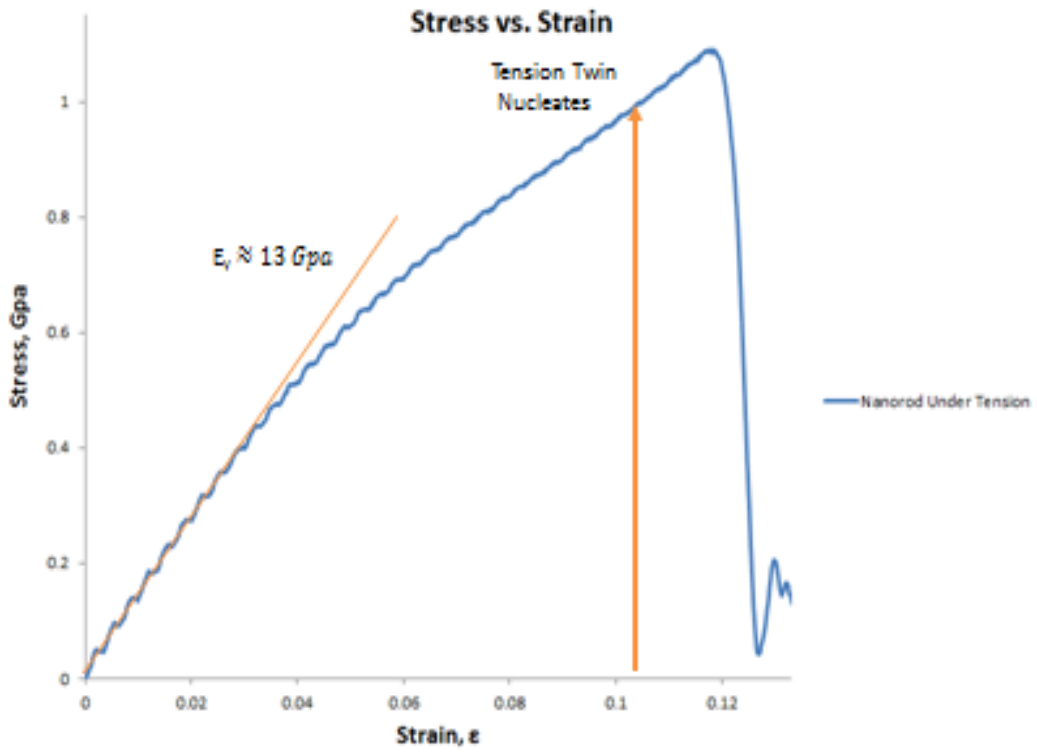


**Figure 26**

Looking at the graph of stress versus strain, one can determine an approximate value for the modulus of elasticity by fitting a curve through the initial linear portion. Taking the slope of the

linear curve the modulus is found to be roughly 13 GPa. The critical point for twin dislocation nucleation occurs at 10% strain and 1 GPa stress, at which point yielding follows shortly at 1.2 GPA. This compares well with the experimental strength testing of a 50 nanometer diameter nanorod, where the elastic modulus was found to be 8 gigapascals and the critical stress for dislocation nucleation occurs at 7-10% strain and 800 megapascal stress[29].

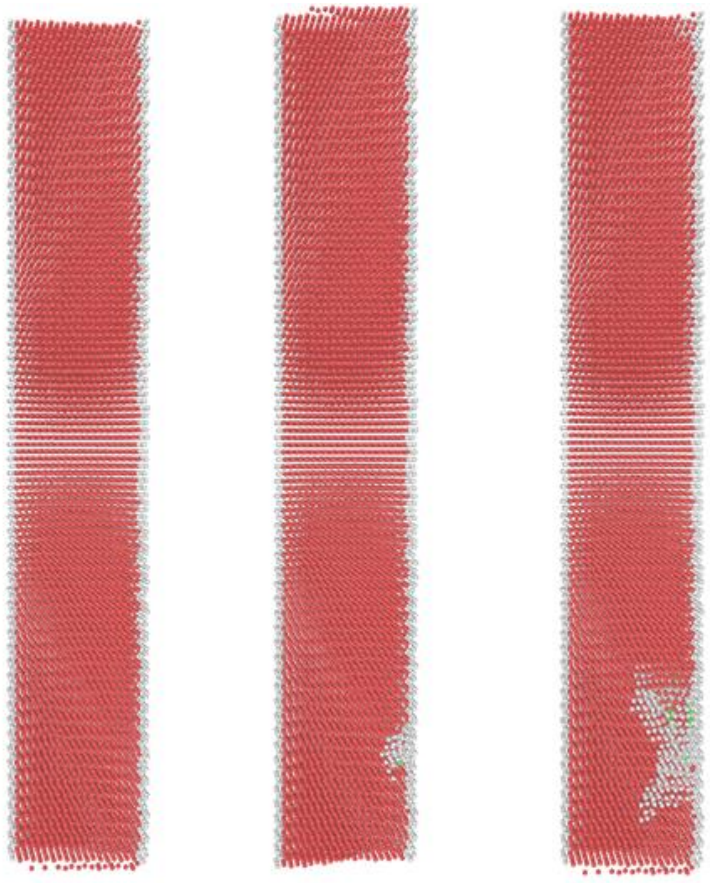

**Figure 27**

Cross sections of the nanorod, at various strains were taken to visualize dislocation motion. Common neighbor analysis displays bulk hcp atoms in pink and dislocation planes in gray. The above images depict $(10\bar{1}0)$ cross sections with a $(10\bar{1}2)$ tension twin dislocation. This agrees

with experiments where the $(10\bar{1}2)$ $[10\bar{1}1]$ twin system forms under plastic deformation[30]. A planar slice was taken for closer analysis of the slip direction for dislocation motion.

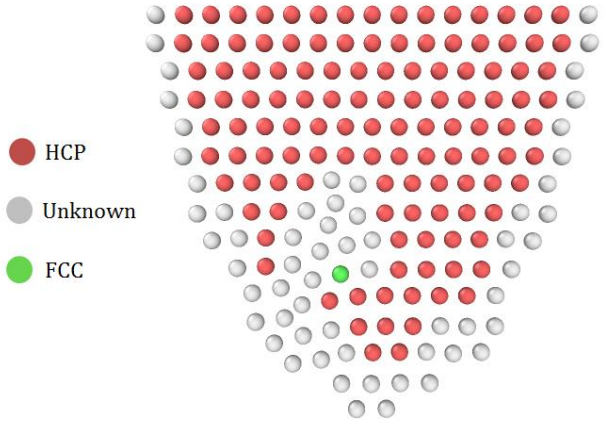


**Figure 28**

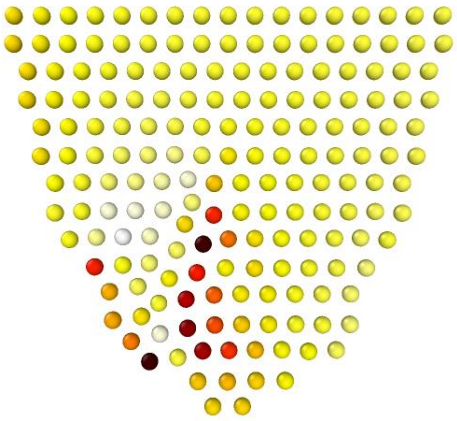

**Figure 29**

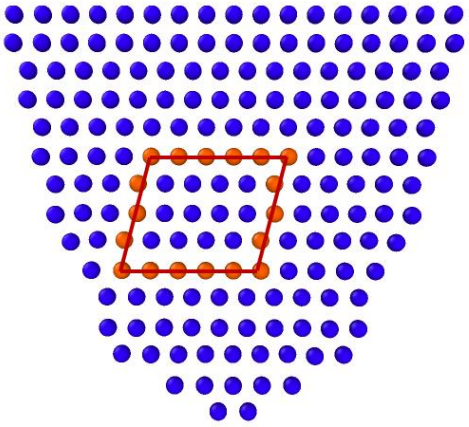

**Figure 30**

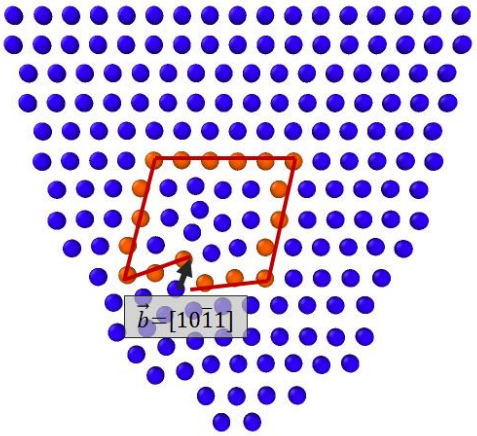


**Figure 31**

Figure 1 depicts the dislocation core using common neighbor analysis, which appears to be composed mostly of screw dislocations. Drawing a burger's circuit and comparing the initial atomic structure before straining to that with a dislocation present, one can obtain a burger's vector as seen in figure 3 and 4. This vector is determined to be in the $[10\bar{1}1]$ direction, which can be most easily seen when atomic displacement is projected onto this direction. Figure 2

shows the magnitude of projection onto the slip direction. Yellow or white atoms indicate small displacement or a perpendicular direction and dark red atoms indicate large displacement or parallel directions. Therefore, the dark red atoms in the dislocation core may be taken as having displaced in the $[10\bar{1}1]$ direction

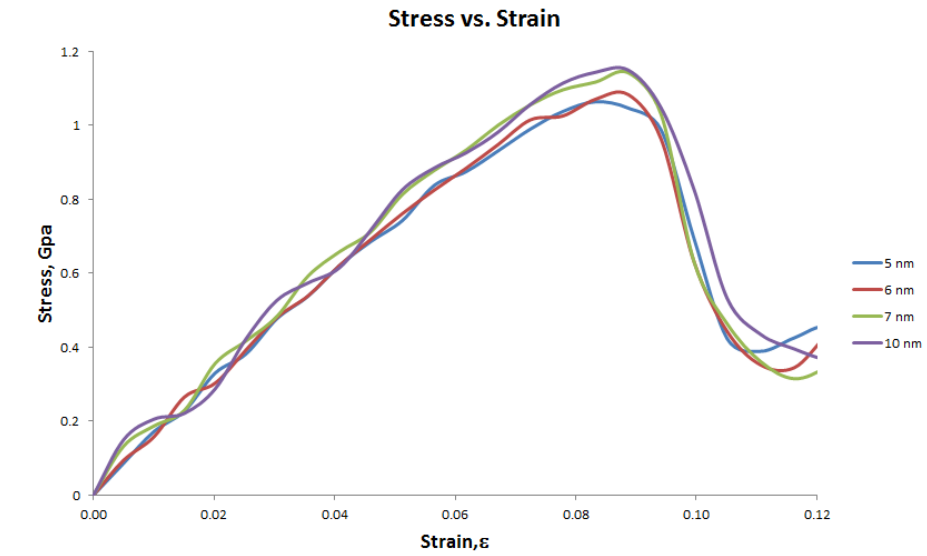


**Figure 32** **Figure 33**

Various size nanorods were run and their dislocation structure was analyzed and found to be similar to that of the 5 nanometer diameter rod. The similarities can also be seen in the elastic modulus and yielding point of the different diameter nanorods. The same twin system is found to form at roughly the same strain and stress in all nanorods with diameters between 5nm and 10nm. For smaller nanorods the percentage of surface atoms is higher, resulting in a

softening effect for the material due to the loss of bonding. As to be expected, yield strength and elastic modulus increases with increasing diameter size because of the smaller percentage of surface atoms relative to the overall total but the plastic deformation mechanism remains unaffected.

# 6. FUTURE EXPLORATION

With computational power doubling once every year according to Moore's law, molecular dynamics will soon be a feasible method for finite size and time simulations. Additionally, progress has been made in recent years to utilize GPUs for computational purposes. GPUs have the advantage over CPUs in that they are designed with graphics processing in mind, which requires a large number of cores for processing. CPUs are limited to roughly 4-8 cores per processor, and then must be linked to allow communication. This communication between CPUs is a costly process and hinders the scalability of large scale parallel processing. Since a single GPU may have thousands of cores present, more efficient and faster processing will be possible in the future. GPU support for the REAM code in LAMMPS will be the next logical step to improve performance and scalability.

# SUMMARY

Limitations in molecular dynamics currently exist for replicating elastic constants and surface properties of HCP and FCC metals. The R-EAM uses a novel approach which more naturally represents electron density distribution in crystal structures. The R-EAM was implemented into LAMMPS existing molecular dynamics program structure, and found to achieve performance only slightly slower to that of existing EAM potentials. Simulations on dislocation dynamics confirm the accuracy of the R-EAM and agree with data obtained from nano-scale strain measurements. Further implementation of R-EAM should allow for great expansion of molecular dynamics because of its increased accuracy in reproducing surface relaxation and dislocation dynamics for HCP and FCC metals.

# APPENDIX A

i. Program Outline

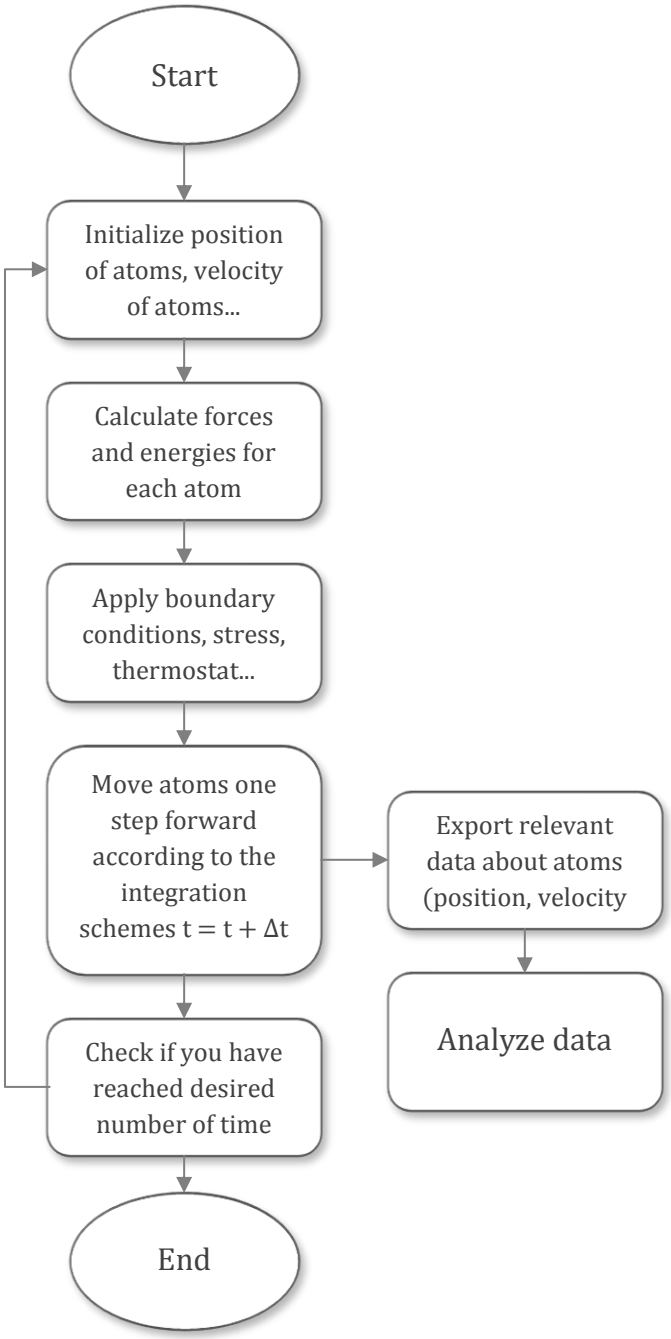


a.

ii. Convergence

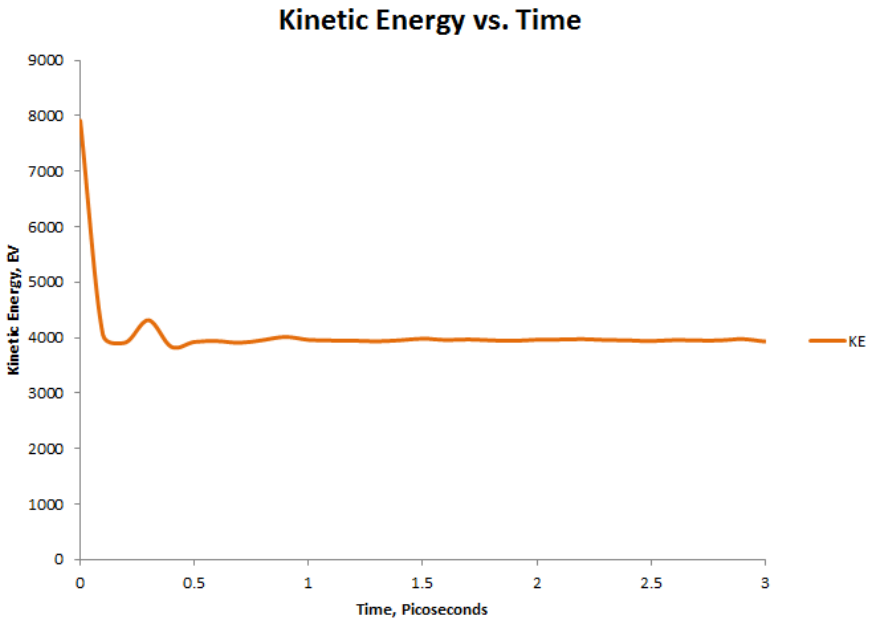
Kinetic Energy vs. Time
Kinetic Energy, EV
9000
8000
7000
6000
5000
4000
3000
2000
1000
0
0
0.5
1
1.5
2
2.5
3
Time, Picoseconds
KE

a.

# WORKS CITED

1. Ashby M. The deformation of plastically non-homogeneous materials. *Philosophical Magazine*. 1970;21(170):399-424.

2. Zhou L, Huang H. Are surfaces elastically softer or stiffer? *Appl Phys Lett*. 2004;84(11):1940-1942.

3. Ozawa M. Universally valid reformulation of the heisenberg uncertainty principle on noise and disturbance in measurement. *Physical Review A*. 2003;67(4):042105.

4. Verlet L. Computer" experiments" on classical fluids. I. thermodynamical properties of lennard-jones molecules. *Physical review*. 1967;159(1):98.

5. Schrödinger E. An undulatory theory of the mechanics of atoms and molecules. *Physical Review*. 1926;28(6):1049.

6. Born M, Oppenheimer R. Zur quantentheorie der molekeln. *Annalen der Physik*. 1927;389(20):457-484.

7. Voter AF. Introduction to the kinetic monte carlo method. In: *Radiation effects in solids.* Springer; 2007:1-23.

8. Newton I, Chittenden N. *Newton's principia: The mathematical principles of natural philosophy.* Daniel Adee; 1848.

9. Lai WM, Rubin DH, Rubin D, Krempl E. *Introduction to continuum mechanics.* Butterworth-Heinemann; 2009.

10. Jones JE. On the determination of molecular fields. II. from the equation of state of a gas. *Proceedings of the Royal Society of London Series A*. 1924;106(738):463-477.

11. Daw MS, Baskes MI. Embedded-atom method: Derivation and application to impurities, surfaces, and other defects in metals. *Physical Review B*. 1984;29(12):6443.

12. Swope WC, Andersen HC, Berens PH, Wilson KR. A computer simulation method for the calculation of equilibrium constants for the formation of physical clusters of molecules: Application to small water clusters. *J Chem Phys*. 1982;76:637.

13. Mott NF, Jones H. *The theory of the properties of metals and alloys.* Courier Dover Publications; 1958.

14. Mattson W, Rice BM. Near-neighbor calculations using a modified cell-linked list method. *Comput Phys Commun*. 1999;119(2):135-148.

15. Hestenes MR, Stiefel E. *Methods of conjugate gradients for solving linear systems*. 1952.

16. Fletcher R, Reeves CM. Function minimization by conjugate gradients. *The computer journal*. 1964;7(2):149-154.

17. Berendsen HJ, Postma JPM, van Gunsteren WF, DiNola A, Haak J. Molecular dynamics with coupling to an external bath. *J Chem Phys*. 1984;81:3684.

18. Nosé S. A unified formulation of the constant temperature molecular dynamics methods. *J Chem Phys*. 1984;81:511.

19. Clausius R. XVI. on a mechanical theorem applicable to heat. *The London, Edinburgh, and Dublin Philosophical Magazine and Journal of Science*. 1870;40(265):122-127.

20. Subramaniyan AK, Sun C. Continuum interpretation of virial stress in molecular simulations. *Int J Solids Structures*. 2008;45(14):4340-4346.

21. Hull D, Bacon DJ. *Introduction to dislocations.* Vol 257. Pergamon Press Oxford; 1984.

22. Kirkwood JG. Statistical mechanics of fluid mixtures. *J Chem Phys*. 1935;3:300.

23. Honeycutt JD, Andersen HC. Molecular dynamics study of melting and freezing of small lennard-jones clusters. *J Phys Chem*. 1987;91(19):4950-4963.

24. Foiles SM, Baskes MI. Contributions of the embedded-atom method to materials science and engineering. *MRS Bull*. 2012;37(05):485-491.

25. Pasianot R, Savino E. Embedded-atom-method interatomic potentials for hcp metals. *Physical Review B*. 1992;45(22):12704.

26. Wan J, Fan Y, Gong D, Shen S, Fan X. Surface relaxation and stress of fcc metals: Cu, ag, au, ni, pd, pt, al and pb. *Modell Simul Mater Sci Eng*. 1999;7(2):189.

27. L.G. Zhou HH. **A response embedded atom method of interatomic potentials**. *Physical Review B*. 2013;87(4).

28. Plimpton S, Crozier P, Thompson A. LAMMPS-large-scale atomic/molecular massively parallel simulator. *Sandia National Laboratories*. 2007.

29. Yu Q, Qi L, Chen K, Mishra RK, Li J, Minor AM. The nanostructured origin of deformation twinning. *Nano letters*. 2012;12(2):887-892.

30. Wonsiewicz BC. *Plasticity of magnesium crystals.* 1966.